Lipid Bilayer Modules as Determinants of K$^+$ Channel Gating*

Ruhma Syeda[1], **Jose S. Santos**[1], **and Mauricio Montal**[2]

From the Section of Neurobiology, Division of Biological Sciences, University of California San Diego, La Jolla, California 92093

Background: Lipid bilayer composition and asymmetry modulate K$^+$ channel function by unknown mechanisms.
Results: Lipid headgroups with exposed hydroxyls on the extracellular facing monolayer stabilize the channel open conformation irrespective of charge.
Conclusion: Stabilization is mediated through a change of interfacial water structure.
Significance: Lipid bilayer asymmetry and its individual monolayers emerge as crucial determinants of K$^+$ channel gating.

The crystal structure of the sensorless pore module of a voltage-gated K$^+$ (Kv) channel showed that lipids occupy a crevice between subunits. We asked if individual lipid monolayers of the bilayer embody independent modules linked to channel gating modulation. Functional studies using single channel current recordings of the sensorless pore module reconstituted in symmetric and asymmetric lipid bilayers allowed us to establish the deterministic role of lipid headgroup on gating. We discovered that individual monolayers with headgroups that coat the bilayer-aqueous interface with hydroxyls stabilize the channel open conformation. The hydroxyl need not be at a terminal position and the effect is not dependent on the presence of phosphate or net charge on the lipid headgroup. Asymmetric lipid bilayers allowed us to determine that phosphoglycerides with glycerol or inositol on the extracellular facing monolayer stabilize the open conformation of the channel. This indirect effect is attributed to a change in water structure at the membrane interface. By contrast, inclusion of the positively charged lysyl-dioleoyl-phosphatidylglycerol exclusively on the cytoplasmic facing monolayer of the bilayer increases drastically the probability of finding the channel open. Such modulation is mediated by a π-cation interaction between Phe-19 of the pore module and the lysyl moiety anchored to the phosphatidylglycerol headgroup. The new findings imply that the specific chemistry of the lipid headgroup and its selective location in either monolayer of the bilayer dictate the stability of the open conformation of a Kv pore module in the absence of voltage-sensing modules.

Voltage-gated channels responsible for cellular excitability are assemblies of modular membrane protein subunits consisting of two distinct, tandemly arranged, functional modules. An N-terminal voltage-sensor module encompassing four transmembrane segments S1–S4 and a C-terminal pore module (PM)[3] con-

sisting of transmembrane segments S5 and S6 (1–4). These modules embody independently folded units of structure (4–7) and function (8–10). The discovery of the voltage-gated K$^+$ (Kv) channel from *Listeria monocytogenes* (KvLm) (11), which embodies an incipient sensor (12), allowed us to dissect the pore module from the intact subunit, to demonstrate that it recapitulates the full complement of functional features after reconstitution in lipid bilayers (8), and to determine its crystal structure in a membrane (5). These advances afford an opportunity to focus on this pore-only entity, extending from the N-terminal end of the S4–S5 linker to the C terminus of the protein, to investigate the role of the individual lipid monolayer components of the bilayer in modulating the channel properties.

It is widely recognized that the lipid bilayer components modulate the function of K$^+$ channels (13–32). A role for lipids on the inactivation of Kv channels, namely the ability of the channel to close and remain closed for prolonged periods while voltage-clamped at an activating potential, has been previously demonstrated (24, 33). In recent years this modulatory effect has been attributed solely to an interaction of the lipid bilayer with the voltage-sensor module. The mechanical properties of the membrane are dictated by its lipid composition and the interaction of the basic charges on the sensor with lipid headgroup phosphates as a means to facilitate sensor movement and therefore pore opening (22, 25).

The crystal structure of the sensorless PM of a Kv channel showed four immobilized lipids filling and surrounding a crevice between subunits at the extracellular surface of the channel, suggesting an affinity for lipids in that region (5). Therefore, we asked if different lipids could act as selective modulators of ion channel function by acting as co-factors in the ion translocation process. Functional studies using single channel current recordings of a sensorless PM reconstituted in symmetric and asymmetric lipid bilayers allowed us to establish the deterministic role of the lipid headgroup on gating the two channel gates

[1] Both authors contributed equally to this work.

[2] To whom correspondence should be addressed: 9500 Gilman Dr., La Jolla, CA 92093. Tel.: 858-534-0931; Fax: 858-822-3763; E-mail: mmontal@ucsd.edu.

[3] The abbreviations used are: PM, pore module; DPhPC, 1, 2-diphytanoyl-*sn*-glycero-3-phosphocholine; DOPC, 1,2-dioleoyl-*sn*-glycero-3-phosphocholine; DPhPE, 1,2-diphytanoyl-*sn*-glycero-3-phosphoethanolamine; DOPA,

1,2-dioleoyl-*sn*-glycero-3-*phosphatidic acid*; DOPG, 1,2-dioleoyl-*sn*-glycero-3-phospho-(1'-rac-glycerol); DPhPG, 1,2-diphytanoyl-*sn*-glycero-3-phospho-(1'-*rac*-glycerol); Lyso-PG, 1-oleoyl-2-hydroxy-*sn*-glycero-3-phospho-(1'-*rac*-glycerol); DOPI, 1,2-dioleoyl-*sn*-glycero-3-phospho-(1'-myo-inositol); lysyl-DOPG, 1,2-dioleoyl-*sn*-glycero-3-[phospho-*rac*-(3-lysyl(1-glycerol))]; monoolein, 1-oleoyl-rac-glycerol; DOPE-PEG$_{350}$, 1,2-dioleoyl-*sn*-glycero-3-phosphoethanolamine *N*-(methoxy(polyethylene glycol)-350); P_o, open probability; γ, single channel conductance; τ_{open}, mean open time; τ_{crit}, τ-critical; t_d, receiver dead time; PG, phosphatidylglycerol.

located at the selectivity filter (34–36), facing the extracellular medium, and at the bundle crossing (37), in direct contact with the cytoplasmic facing leaflet of the membrane.

Taking advantage of the uniqueness of asymmetric bilayers (38–42) allowed us to uncover two mechanisms for the stabilization of the open channel conformation. First, we discovered that the inclusion of lipids with headgroups that coat the extracellular membrane-solution interface with hydroxyl groups such as those found in glycerol, phosphoglycerol, phosphoinositol, and lysyl-phosphoglycerol increased drastically the probability of finding the channel open. This effect was observed to be independent of headgroup charge, number of acyl chains, and whether the chains were methyl branched or not. We propose that the stabilizing effect of these surface-coating hydroxyls is indirectly mediated by an interaction with water at the membrane-solution interface. We further validate this proposal by demonstrating that the addition of 1% (0.17 M) ethylene glycol or 0.2 M mannitol to the extracellular bathing solution of lipid bilayers lacking exposed hydroxyls emulates the gain in open conformation stability observed when lipids with exposed hydroxyls are present at the extracellular membrane interface. Second, we unveiled a π-cation interaction (43) between a lysine containing lipid headgroup and a conserved aromatic residue in Kv channels at the protein cytoplasmic surface as an additional stabilizer to generate an open, rarely interrupted, K$^+$ permeation path.

The new findings provide evidence that the PM of Kv channels may be transformed into an open conductor through interactions with lipid modulators that target either the filter gate, through a destabilization of water structure, or the bundle gate, via a direct interaction, and thereby stabilize the conducting conformation of the channel. The implication is that lipids are crucial not only for proper protein folding (44) but also to modulate, in a deterministic manner, the properties of the channel.

EXPERIMENTAL PROCEDURES

Protein Expression and Purification—KvLm PM, WT, and mutants were expressed in *Escherichia coli* XL1-Blue with a C-terminal His tag and purified by Ni^{2+}-affinity and size exclusion chromatography as previously described (45). Single channel mutations were introduced using the QuikChange site-directed mutagenesis kit (Agilent) according to the manufacturer's instructions.

Liposome Preparation and Protein Reconstitution—Liposomes were composed of 100 mol % of 1,2-diphytanoyl-*sn*-glycero-3 phosphocholine (DPhPC), 1,2-dioleoyl-*sn*-glycero-3-phosphocholine (DOPC), 1,2-diphytanoyl-*sn*-glycero-3-phosphoethanolamine (DPhPE), or 90 mol % of DPhPC and 10 mol % of the indicated test lipids: DOPC, DPhPE, 1,2-dioleoyl-*sn*-glycero-3-phosphatidic acid (DOPA), 1,2-dioleoyl-*sn*-glycero-3-phospho-(1′-rac-glycerol) (DOPG), 1,2-diphytanoyl-*sn*-glycero-3-phospho-(1′-*rac*-glycerol) (DPhPG), 1-oleoyl-2-hydroxy-*sn*-glycero-3-phospho-(1′-*rac*-glycerol) (lyso-PG), 1,2-dioleoyl-*sn*-glycero-3-phospho-(1′-myo-inositol) (DOPI), 1,2-dioleoyl-*sn*-glycero-3-[phospho-*rac*-(3-lysyl(1-glycerol))] (lysyl-DOPG), 1-oleoyl-rac-glycerol (monoolein) and 1,2-dioleoyl-*sn*-glycero-3-phosphoethanolamine *N*-(methoxy-(polyethylene glycol))-350 (DOPE-PEG$_{350}$) (Avanti Polar

Lipids, Alabaster, AL) (Fig. 1). Liposomes were prepared as previously described (45). When indicated, ethylene glycol (0.17 M) or mannitol (0.2 M) were supplemented to the rehydrated liposome suspension prior to extrusion. For reconstitution, the protein was diluted ~100–300-fold into preformed liposomes to give final protein concentrations 2–5 μg/ml. The proteoliposomes were incubated on ice for 15 min prior to bilayer recording experiments. Fresh aliquots of liposomes and protein were used for every experiment.

Single Channel Recordings Using Droplet Interface Lipid Bilayers—Single channel currents were recorded from droplet interface bilayers as described (10, 46). Briefly, a 10 × 10 × 4-mm Plexiglas chamber was filled with hexadecane (Sigma) containing 1 mol % of DPhPC. A 0.2-mm diameter Ag/AgCl wire electrode (40 mm in length) was attached to each of two micromanipulators (NMN-21, Narishige, Japan). Droplets (~200 nl) were placed with a pipette on each of the electrodes, which had been coated with 3% (w/v) low-melt agarose (65 °C). The electrode carrying the droplet with the proteoliposomes in 0.5 M KCl, 10 mM HEPES, pH 7.4, was connected to the grounded end (*cis* side) of the amplifier head-stage. The second electrode, in a droplet containing exclusively liposomes in the same buffer, was connected to the working end of the head-stage (*trans* side). The chamber, electrodes, and the amplifier head-stage were enclosed in a Faraday cage. The droplets were incubated in hexadecane containing 1 mol % of DPhPC until a monolayer of lipid had formed around them (~5 min). A bilayer spontaneously formed when the two droplets were brought into contact.

Regardless of bilayer composition, and symmetric or asymmetric configuration, the proteoliposome droplet was always placed on the *cis* compartment to ensure that the filter gate of the channel protein remained on the *cis* side and was exposed to only one class of lipids. To confirm the orientation of the protein in the reconstituted bilayers with the consequent outward flow of current (from bundle to filter), the open channel blocker tetrabutyl ammonium was used (45). Tetrabutyl ammonium stocks (5 mM) were made in droplet solution (0.5 M KCl, 10 mM HEPES, pH 7.4) and injected into the bundle-facing droplet (*trans* side) at the end of each experiment to a final concentration of 50 μM using a Nano injector (VWR instrument). In all configurations, channel orientation was verified by sided tetrabutyl ammonium block. The test lipids were always supplemented at 10 mol % in 90 mol % of DPhPC. To increase the signal-to-noise ratio all electrical measurements were performed in 0.5 M KCl, 10 mM HEPES, pH 7.4, at 100 mV and 22 ± 2 °C, unless otherwise indicated.

Single Channel Acquisition and Analysis—Single channel currents were sampled at 20 kHz using an Axon 200B patch clamp amplifier, filtered by using a low pass Bessel filter (80 dB/decade) with a corner frequency of 2 kHz, and then digitized with a DigiData 1320 A/D converter (Axon Instruments). All pre-processing and analysis of the single channel recordings was performed with QuB software. Currents in symmetric lysyl-DOPG were further filtered to 400–700 Hz, whereas additional off-line filtering of 2 kHz was used for all other recordings. Event detection was performed by time course fitting with the segmental *k*-means algorithm (SKM) (47). Stretches of the
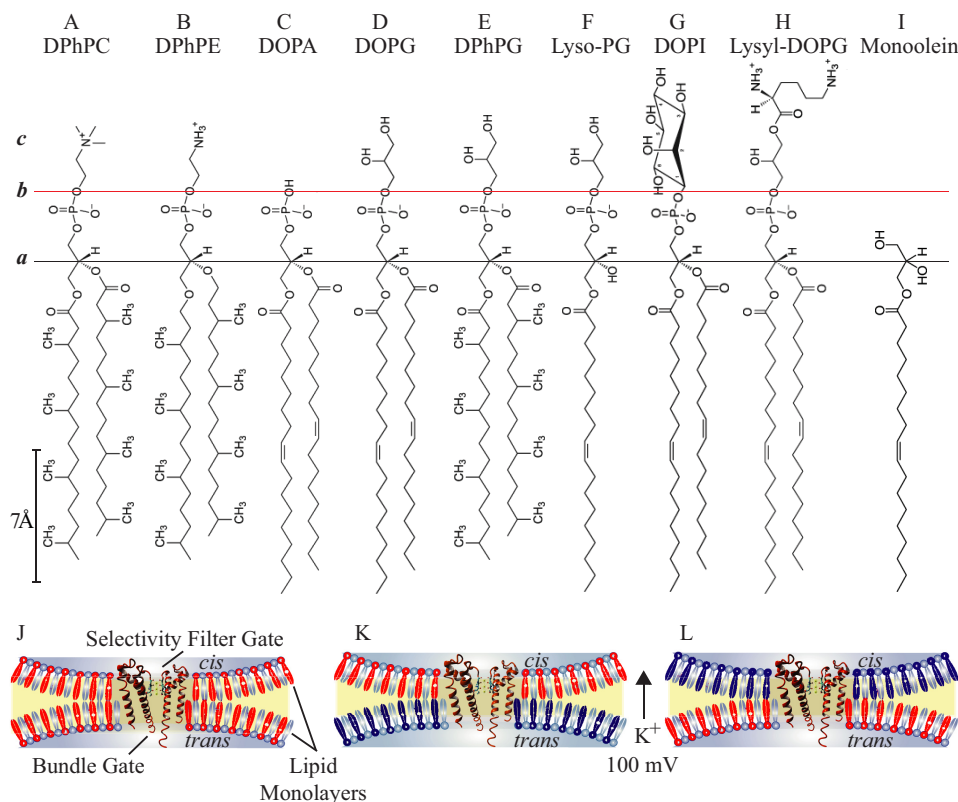
FIGURE 1. **Chemical structures of lipid molecules and bilayer configurations.** *Horizontal black line* designates the common acyl-glycerol esterification site in all the lipids (plane *a*). *Horizontal red line* indicates a shared negatively charged phospho-X headgroup boundary, where *X* bears distinct head group chemistry (plane *b*): *A*, phosphocholine; *B*, phosphoethanolamine; *C*, phosphatidic acid; *D–F*, phosphoglycerol; *G*, phosphoinositol; *H*, lysyl-phosphoglycerol. *c*, denotes a layer with interfacial properties generated by the specific headgroup chemistry. *I–K*, schematic representation of the PM (*orange*) in a lipid bilayer (*blue* contour) depicting the orientation of the selectivity filter and bundle gates of the PM in symmetric (*I*) and asymmetric (*J* and *K*) bilayers. DPhPC is depicted in *cyan*, doping lipids are in *red* and *dark blue*, irrespective of charge.

recordings in which the channel was closed were included in the analysis; hence, the calculated P_o is proportional to the ratio of open time/total time of the recording. Segments of continuous recordings in the range of 30 s $\leq t \leq$ 400 s were used for analysis. To avoid the detection of erroneous events, the receiver dead time (t_d) was set at 300 μs for all recordings except for PM in symmetric lysyl-DOPG for which the t_d was set to 700–1000 μs. Accordingly, transitions shorter than the t_d were ignored; transitions longer than the t_d were accepted as "events." To calculate the median burst length, bursts were defined as a group of three or more opening transitions with intraburst closures shorter than τ-critical (τ_{crit}) and terminated by an interburst closure longer than τ_{crit}. The value of τ_{crit} was calculated from the closed dwell time histograms in QuB for each record (3 ms $\leq \tau_{crit} \leq$ 20 ms). All the results reported were done at least in triplicate; the calculated values are reported as mean $\pm$ S.E. **N** and ***n*** denote the number of events and number of experiments, respectively. Statistical significance was assessed using the unpaired, two-tailed Student's *t* test. Wherever the statement "equal within error" appears, the *p* value was >0.05, indicating that the two groups in question are equal and there is no significant statistical difference. By contrast, wherever the open probability (or any other parameter) is stated to be "x-fold higher," the *p* value was <0.05 indicating that the differences are statistically significant.

Identification of KvLm PM Residues Exposed to Lipid Headgroups at the Membrane Interface—To determine which residues in the PM are within 5 Å of a lipid phosphate or choline headgroup we used YASARA (Yasara Bioscience) to run a 10 ns molecular dynamics simulation (48) of KvLm PM (5) in DOPC bilayers. At the end of the simulation, residues within 5 Å of a phosphate oxygen or a choline nitrogen were identified, given that the Debye screening at 0.5 M salt is 4 Å. The simulation was performed at 25 °C and pH 7.4 with the salt concentration fixed at 0.5 M KCl. The AMBER03 force-field was employed (49).

RESULTS

The Glycerol Moiety on the Phosphoglyceride Headgroup, and Not the Charge, Dictates the Channel Open Probability—To investigate the functional consequence of an interaction between the PM of a Kv channel and the surrounding lipids, PM function was screened in lipid bilayers with varying headgroup chemistry and acyl chains (Fig. 1). The sensorless PM of KvLm was reconstituted in droplet interface bilayers in which both cytoplasmic and extracellular leaflets were of equal composition (symmetric bilayers, Fig. 1*J*); channel function was assayed by monitoring the single channel steady-state activity at a depolarizing potential of 100 mV while bathing both sides of the membrane in 0.5 M KCl. Channel function was first assayed in 100 mol % of DPhPC, DOPC, or DPhPE. In these bilayers of zwitterionic phospholipid composition, no channel activity was observed

Modulation of K+ Channel Gating by Lipids
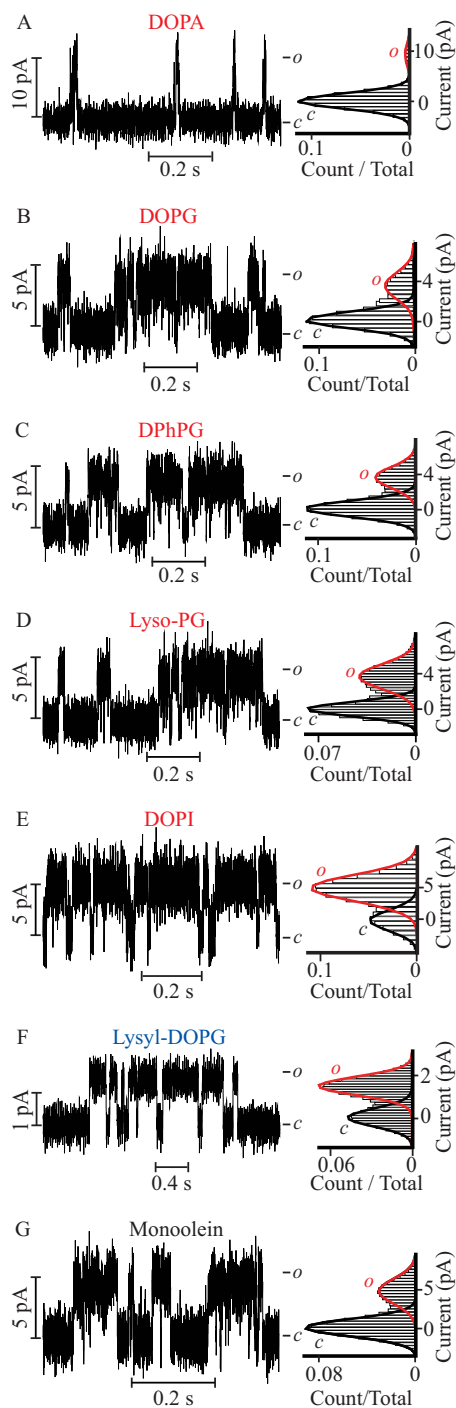
FIGURE 2. The PM exhibits characteristic lipid-dependent gating in symmetric bilayers. Single channel steady-state current recordings (*left*) and their corresponding normalized all point histograms (*right*) of the PM in symmetric DPhPC bilayers supplemented with the following lipids: *A,* DOPA; *B,* DOPG; *C,* DPhPG; *D,* lyso-PG; *E,* DOPI; *F,* lysyl-DOPG; and *G,* monoolein. All the recordings were acquired at V = 100 mV, except for bilayers supplemented with lysyl-DOPG, which were acquired at V = 150 mV.

TABLE 1

Single channel properties of the PM in symmetric DPhPC lipid bilayers supplemented with the indicated lipids

Experimental conditions	γ	P_o	τ_{open}	Burst length	N
	pS		*ms*	*ms*	*n*
DOPA	105 ± 4	0.06 ± 0.01	1.1 ± 0.2	4 ± 1	20,200 *5*
DOPG	42 ± 2	0.29 ± 0.04	2.6 ± 0.1	20 ± 4	9,663 *3*
DPhPG	42 ± 3	0.35 ± 0.06	5.8 ± 0.9	16 ± 2	9,887 *3*
Lyso-PG	40 ± 2	0.36 ± 0.03	3.7 ± 0.4	18 ± 2	15,859 *4*
DOPI	49 ± 4	0.61 ± 0.08	2.8 ± 0.4	15 ± 3	18,541 *4*
Lysyl-DOPG	10 ± 2	0.59 ± 0.08	16 ± 2	40 ± 5	10,620 *4*
Monoolein	60 ± 7	0.32 ± 0.03	2.7 ± 0.6	12 ± 3	8,689 *4*

in DOPA-supplemented bilayers was further characterized by a brief mean open time (τ_{open}) followed by immediate closures ($\tau_{open} = 1.1 \pm 0.2$ ms, burst length = 4 ± 1 ms), thereby defining a very low open probability (P_o) of 0.06 ± 0.01 (Table 1). Comparison of the structures of the lipid headgroups (Fig. 1) suggests that the choline or ethanolamine moieties in DPhPC or DPhPE hinder PM activity. To test this hypothesis, we replaced the terminal choline with a glycerol moiety and measured channel activity in bilayers supplemented with the negatively charged lipids DOPG (Fig. 2*B*) or DPhPG (Fig. 2*C*). It is worth noting that the glycerol moiety in the headgroup of DOPG and DPhPG (plane "*c*," Fig. 1) is different from the glycerol backbone to which the acyl chains are attached (plane "*a*," Fig. 1). In DOPG-supplemented bilayers, the P_o was 0.29 ± 0.04, a ~5-fold increase relative to the P_o measured in DOPA containing bilayers. In close agreement, the P_o in DPhPG-supplemented bilayers also increased by ~6-fold to 0.35 ± 0.06. In both phosphatidylglycerol (PG) containing bilayers, the PM opened to a lower γ (42 ± 2 and 42 ± 3 pS) but remained open for significantly longer times in both DOPG ($\tau_{open} = 2.6 \pm 0.1$ ms and burst length = 20 ± 4 ms) and in DPhPG-supplemented bilayers ($\tau_{open} = 5.8 \pm 0.9$ ms and burst length = 16 ± 2 ms) (Table 1). This result suggests that the terminal glycerol moiety (plane *c*, Fig. 1) accounts for stabilization of the conductive conformation of the PM. Next, we queried whether the terminal glycerol was sufficient to produce the observables by assaying PM function in a lipid bilayer doped with negatively charged lyso-PG, a lipid that retains the same headgroup but contains only one acyl chain (Fig. 2*D*). In lyso-PG containing bilayers, the PM exhibits a $\gamma = 40 \pm 2$ pS and $P_o = 0.36 \pm 0.03$, values equal within error to those observed in DOPG and DPhPG as are the values of $\tau_{open} = 3.7 \pm 0.4$ ms and burst length = 18 ± 2 ms (Table 1). These results indicate that stabilization of the PM open conformation relies on the presence of a glycerol moiety in the headgroup of the doping lipid (plane *c*, Fig. 1) but not on the headgroup charge (plane "*b*," Fig. 1), number of acyl chains (plane *a*, Fig. 1), or methyl branching of acyl chains (Fig. 1).

To discern if this effect was specific to glycerol, we tested the activity in bilayers supplemented with negatively charged DOPI (Fig. 2*E*), a lipid that replaces the two free hydroxyl groups of

($n \geq 20$, 10, and 15, respectively). Next, we assayed the PM activity in symmetric bilayers composed of 90 mol % of DPhPC supplemented with 10 mol % of test lipids (Fig. 1). Remarkably, when DPhPC bilayers were supplemented with the negatively charged DOPA, the PM was observed to open frequently with a single channel conductance (γ) = 105 ± 4 pS (Fig. 2*A*). Activity
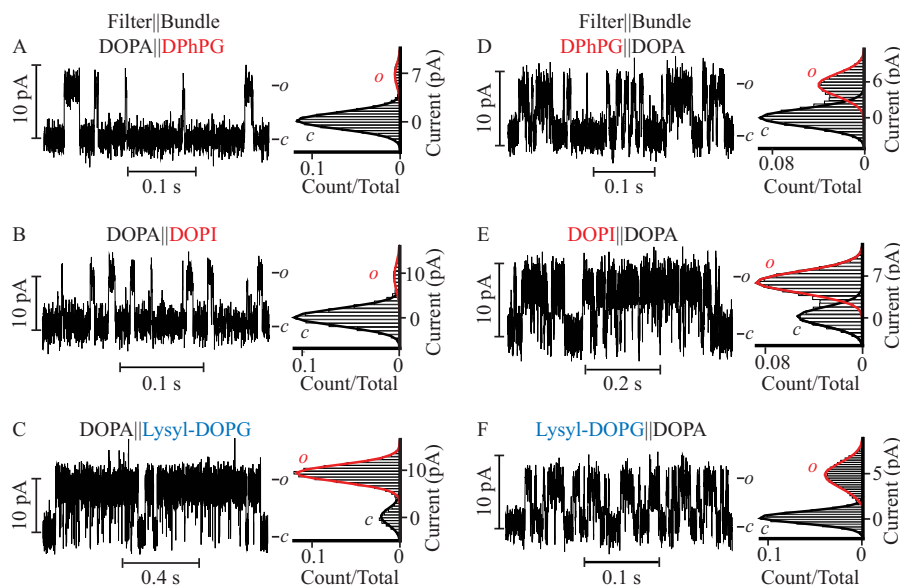
FIGURE 3. **Lipid bilayer asymmetry strongly dictates the PM channel characteristics.** Steady-state single channel current recordings (*left*) and their corresponding currents normalized all point histograms (*right*) of the PM reconstituted in asymmetric DPhPC bilayers in which the DOPA-containing mono-layer colocalizes with the filter gate and DPhPG (*A*), DOPI (*B*), lysyl-DOPG-containing monolayers (*C*) are assigned a location corresponding to that of the bundle facing compartment. The orientation of the corresponding lipid monolayers was reversed in *D–F* such that the DOPA-containing monolayer colocalizes with the bundle gate and the test lipid with the filter gate.

glycerol with a sugar thereby increasing the number of terminal hydroxyls presumably exposed to the bulk solution to five. When reconstituted in DOPI containing bilayers the PM opens to a γ equal within error to that observed in the PG containing bilayers (49 ± 4 pS), yet resides in the open state for twice as long ($P_o = 0.61 \pm 0.08$) as compared with that in the PG-supplemented bilayers (Table 1). This represents a 10-fold increase in finding the PM open relative to the DOPA-containing bilayers. These results establish that a layer of hydroxyl groups at the membrane-aqueous solution interface (plane *c*, Fig. 1) favors the open conformation of the PM.

Next, we asked if it was necessary for the hydroxyls to be at the most exposed terminal position by testing PM activity in bilayers supplemented with the positively charged lysyl-DOPG or with the neutral monoolein (Fig. 2, *F* and *G*). In bilayers containing lysyl-DOPG, a lipid to which a lysine group has been added to the terminal glycerol of DOPG (Fig. 1), the PM opened to a high P_o (0.59 ± 0.08), arising from the longest uninterrupted openings ($\tau_{open} = 16 \pm 2$ ms and burst length = 40 ± 5 ms) of lowest amplitude ($\gamma = 10 \pm 2$ pS) (Fig. 2*F* and Table 1). In monoolein containing bilayers, a single acyl chain glyceride lacking a phosphoglycerol moiety but still carrying a terminal hydroxyl group (plane *a*, Fig. 1), the PM exhibited an intermediate γ of 60 ± 7 pS and a P_o (0.32 ± 0.03) (Fig. 2*G* and Table 1) equal within error to that observed in other PG containing bilayers (Fig. 2, *B–D*).

Together, these results demonstrate that: 1) the hydroxyl need not be at a terminal position (plane *c*, Fig. 1) to stabilize the channel open conformation; 2) the effect is not dependent on the presence of phosphate (plane *b*, Fig. 1); 3) charge on the lipid headgroup is not a determinant (planes *b* and *c*, Fig. 1); and 4) there is an additional stabilization of the open conformation of the PM when a positively charged terminal lysyl moiety is added to the PG headgroup (plane *c*, Fig. 1).

The Lysyl Moiety on the Cytoplasmic Facing Monolayer Headgroup Stabilizes the Open Conformation—To determine the contribution of the cytoplasmic facing monolayer to the pore function, channel activity was assayed in three types of asymmetric bilayers (Fig. 1, *K* and *L*): with 10 mol % of DOPA on the extracellular facing monolayer in which the PM filter gate is located, and 10 mol % of DPhPG, DOPI, or lysyl-DOPG on the intracellular facing monolayer, assigned to the PM bundle gate location by tetrabutyl ammonium block (45) (Fig. 3, *A–C*). When reconstituted into a bilayer supplemented with DOPA on the extracellular facing monolayer, and with DPhPG in the cytoplasm facing monolayer (DOPA‖DPhPG), the probability of finding the channel open was 0.07 ± 0.01 (Fig. 3*A* and Table 2), a value equal within error to that observed when the PM was reconstituted in symmetric DOPA containing membranes (0.06 ± 0.01). When DOPI replaced DPhPG as the doping lipid at the cytoplasmic monolayer (DOPA‖DOPI), the P_o was 0.05 ± 0.02 (Fig. 3*B*). In contrast, when lysyl-DOPG was introduced into the cytoplasmic monolayer (DOPA‖lysyl-DOPG) the P_o was 0.55 ± 0.09 (Fig. 3*C*, Table 2), a value equal within error to that observed in symmetric lysyl-DOPG containing bilayers. These results indicate that the high open probability observed in symmetric lysyl-DOPG containing bilayers can be attributed solely to the confinement of this lipid on the cytoplasmic lipid monolayer. The results also indicate that it is the lysyl moiety (plane *c*, Fig. 1) in lysyl-DOPG and not the glycerol and inositol moieties (plane *c*, Fig. 1) of lipids facing the cytoplasm that promotes this state of high P_o. The observed ~6-fold increase in τ_{open} and ~8-fold increase in burst duration, when lysyl is present as the terminal moiety in the lipid headgroup, indicate that the 10-fold increase in P_o observed in DOPA‖lysyl-DOPG containing bilayers *versus* DOPA‖DOPA-supplemented bilayers is due to a stabilization of the open conformation of the PM (Tables 1 and 2).

TABLE 2

Single channel properties of the PM in asymmetric DPhPC lipid bilayers supplemented with the indicated lipids at either the filter or the bundle facing compartments

Experimental conditions (Filter‖bundle)	γ	P_o	τ_{open}	Burst length	N
	pS		*ms*	*ms*	*n*
DOPA‖DPhPG	74 ± 4	0.07 ± 0.01	1.8 ± 0.4	3 ± 1	8,674
					5
DOPA‖DOPI	94 ± 3	0.05 ± 0.02	1.9 ± 0.2	4 ± 1	4,614
					4
DOPA‖lysyl-DOPG	92 ± 7	0.55 ± 0.09	5.5 ± 0.9	30 ± 5	19,403
					5
DPhPG‖DOPA	50 ± 5	0.33 ± 0.04	2.9 ± 0.6	10 ± 1	11,674
					3
DOPI‖DOPA	70 ± 4	0.5 ± 0.1	6.2 ± 0.9	11 ± 2	10,147
					4
Lysyl-DOPG‖DOPA	46 ± 2	0.35 ± 0.04	2.5 ± 0.4	9 ± 2	14,491
					6

The Lysyl Moiety in Lysyl-DOPG Stabilizes the Open Conformation through a Direct Interaction with a Phenylalanine Residue in the PM—Because we could ascribe the lipid effect at the cytoplasmic leaflet to the positive charge of the lysyl headgroup, we searched for negatively charged residues in the PM sequence that could be exposed at the intracellular monolayer-solution interface. This search failed to find such a residue; therefore, we asked if there were any other residues that were lipid exposed and that could have an affinity for the lysyl charge at the membrane surface. To identify candidate PM residues interacting with lipid headgroups, the 3.1-Å resolution PM structure obtained in a lipid membrane (Protein Data Bank code 4H33) (5) was energy minimized in a DOPC bilayer bathed in 0.5 M KCl at pH 7.4 and subjected to a 10-ns molecular dynamic simulation. At the end of the simulation, residues at the interface between the hydrophobic core of the bilayer and the hydrophilic exterior located within 5 Å from phosphate oxygen or from the choline nitrogen in DOPC were identified. This analysis discerned only one residue: Arg-18 located at the cytoplasmic end of the outer helix (S5 in KvLm full-length). To test the contribution of Arg-18 to the stabilizing effect, we assayed the function of the R18D mutant in symmetric DOPA and lysyl-DOPG containing bilayers (Fig. 4, *A* and *B*). In DOPA, R18D opened with a P_o of 0.06 ± 0.02, whereas in lysyl-DOPG it opened to a P_o of 0.5 ± 0.1. In both types of bilayers the P_o of R18D was equal within error to that of WT (Table 1), we conclude that Arg-18 did not account for the observed high P_o in the WT.

Because we have not yet crystallized the open conformation of the PM, and expecting the position of residues surrounding the bundle crossing to change from that observed in the structure of the closed conformation, we asked if there was a residue at a position adjacent to that of Arg-18 that could form a strong interaction with the lysyl group. We surmised that the phenylalanine at position 19 might do the job by forming a π-cation (43) interaction with lysyl in the open conformation. To test this hypothesis, we expressed a PM mutant (F19L) that best retains the side chain volume and hydrophobicity of phenylalanine, but cannot form the predicted π-cation interaction. F19L opened to a higher P_o in DOPA containing bilayers (0.17 ± 0.03) (Fig. 4C) and to a lower P_o (0.21 ± 0.02) in lysyl-DOPG-supplemented bilayers (Fig. 4D) than WT, indicating that Phe-19 stabilizes the closed conformation in DOPA containing bilayers, as well as the open conformation in lysyl-DOPG con-
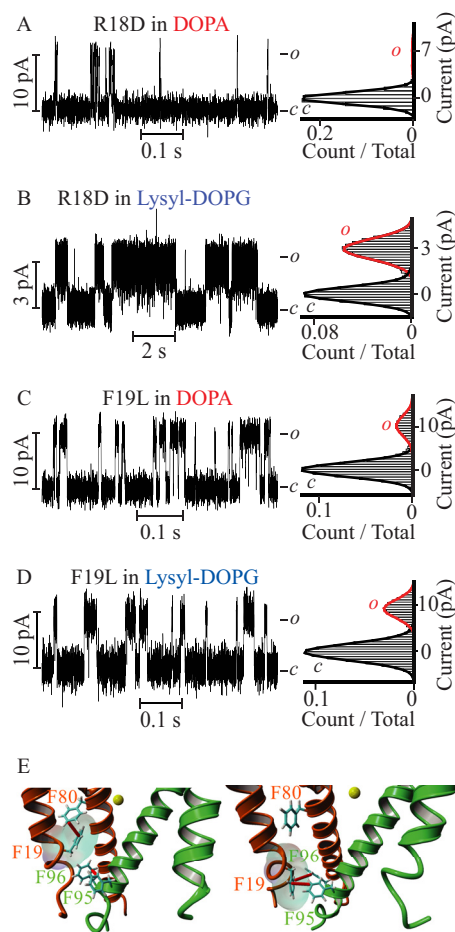

FIGURE 4. **The R18D PM mutant is sensitive to lysyl-DOPG but the F19L PM mutant is not.** Steady-state current recordings of R18D (*A* and *B*) and F19L (*C* and *D*) mutant PMs reconstituted in symmetric DOPA containing bilayers (*A* and *C*) and lysyl-DOPG supplemented bilayers (*B* and *D*). The R18D channel parameters are γ = 65 ± 7 pS, P_o = 0.06 ± 0.01 in DOPA containing bilayers, and γ = 20 ± 5 pS, P_o = 0.5 ± 0.1 in lysyl-DOPG-supplemented bilayers. The F19L channel parameters are γ = 101 ± 2 pS, P_o = 0.17 ± 0.03 in DOPA containing bilayers, and γ = 91 ± 2 pS, P_o = 0.21 ± 0.02 in lysyl-DOPG-supplemented bilayers. All recordings were acquired at V = 100 mV, except for those shown in *B*, which were recorded at V = 100 mV. *E*, Phe-19 participates in an intrasubunit π-π interaction with Phe-80 (*left panel*) or an intersubunit π-π interaction with Phe-95 and Phe-96 (*right panel*) to stabilize the closed conformation of the channel. Only two adjacent subunits (*orange* and *green*) are depicted, focusing on the bundle gate facing the cytoplasmic compartment (PDB code 4H33) (5). *Yellow sphere* depicts a K$^+$ ion at the selectivity filter S4 binding site. Phe residues involved in π-π interactions (*red*) are represented by *sticks* and numbered according to the KvLm sequence (5).

taining bilayers, in agreement with our prediction. The stabilization of the closed state by Phe-19 in the WT can be reasoned by noting that, in the closed conformation of the PM observed at the end of the molecular dynamic simulation, this residue can make one of two π-π interactions (50): an intrasubunit interaction with Phe-80 or an intersubunit interaction with Phe-95 and Phe-96, all in the inner helix (S6 in the full-length) (Fig. 4E). These results suggest that a π-cation interaction between Phe-19 in the PM and the lysyl moiety in lysyl-DOPG accounts for the observed stabilization of the open conformation of the PM in bilayers having lysyl-DOPG in the lipid monolayer facing the cytoplasm.

Glycerol or Inositol on the Extracellular Facing Monolayer Headgroup Stabilizes the Open Conformation—To dissect the contribution of the extracellular facing monolayer to the pore function, channel activity was assayed in three types of asymmetric bilayers (Fig. 1, K and L): bilayers supplemented with DPhPG, DOPI, or lysyl-DOPG on the extracellular facing monolayer and with DOPA on the intracellular facing monolayer (Fig. 3, D–F). When DPhPG was present on the extracellular facing leaflet (DPhPG∥DOPA), the P_o was 0.33 ± 0.04 (Fig. 3D and Table 2), a value that is equal within error to that measured when DPhPG was introduced in both leaflets (0.35 ± 0.06), and 6-fold larger than reported in symmetric DOPA-supplemented bilayers. When DOPI replaced DPhPG (DOPI∥DOPA) (Fig. 3E and Table 2), the P_o increased to 0.5 ± 0.1, a value equal within error to that observed in DOPI containing symmetric bilayers (0.61 ± 0.08) and 10-fold higher than reported in DOPA∥DOPA-supplemented bilayers. In contrast, when lysyl-DOPG was added to the extracellular facing monolayer (lysyl-DOPG∥DOPA) (Fig. 3F and Table 2) the P_o was 0.35 ± 0.04, a value equal within error to that observed in DPhPG∥DOPA-supplemented bilayers, but lower than the P_o in symmetric lysyl-DOPG-supplemented bilayers (0.59 ± 0.08). These results demonstrate that the high P_o determined in symmetric DPhPG and DOPI containing bilayers, but not in lysyl-DOPG-supplemented bilayers, can be fully reproduced by inclusion of these lipids exclusively in the extracellular facing leaflet. Together, these results point to the propitious role of the glycerol and inositol moieties on the lipid headgroup (plane c, Fig. 1) facing the extracellular leaflet in inducing an increase in P_o that is well correlated with an increase in τ_{open} and burst length (Table 2). Thus, the presence of these lipids at the extracellular surface stabilizes the open conformation of the pore.

Glycerol or Inositol on the Extracellular Facing Monolayer Stabilizes the Open Conformation through an Indirect Interaction with the PM Filter Gate, a Water Structure-mediated Effect?—Having posited that the crucial lipid structural element for stabilization of the PM open conformation on the extracellular facing monolayer is a layer of hydroxyl groups exposed at the bilayer-aqueous solution interface (plane a for monolein, plane c for DOPI and all PG lipids, Fig. 1), we asked what physical property of the interface was being modulated. The realization that glycerol and sugars are commonly used as cryoprotectants suggests that hydroxyls at the membrane interface may alter the structure of water (51–53). To test this hypothesis, we utilized a negatively charged phospho-
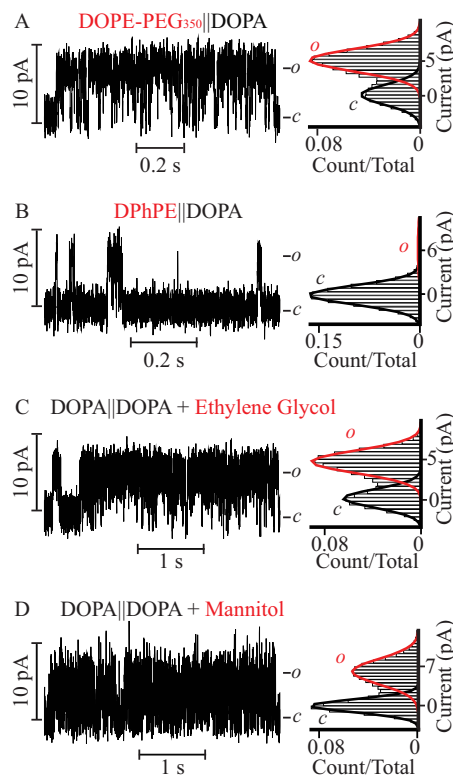
FIGURE 5. **A cryoprotectant at the extracellular monolayer stabilizes the PM open state.** Single channel steady-state current recordings (*left*) and their corresponding normalized all point histograms (*right*) of the PM in asymmetric lipid bilayers (*A* and *B*) with a lipid anchored cryoprotectant (*A*) DOPE-PEG$_{350}$ or (*B*) DPhPE-containing monolayers colocalized with the filter gate and the DOPA-containing monolayer with the bundle gate. The distinct channel parameters are: $\gamma = 55 \pm 5$ pS, $P_o = 0.61 \pm 0.03$, $\tau_{\text{open}} = 4.1 \pm 0.4$ ms and burst length = 16 ± 2 ms for A and $\gamma = 62 \pm 3$ pS, $P_o = 0.04 \pm 0.01$, $\tau_{\text{open}} = 1.2 \pm 0.2$ ms and burst length = 5 ± 1 ms for B. Single channel steady-state current recordings (*left*) and their corresponding normalized all point histograms (*right*) of the PM in DOPA-containing symmetric lipid bilayers bathed in 0.5 M KCl on the PM bundle side and in 0.5 M KCl, 1% ethylene glycol (*C*) or 0.5 M KCl, 0.2 M mannitol (*D*) on the filter gate.

glyceride with an ethanolamine moiety (PE) anchored to a polyethylene glycol (PEG)$_{350}$ chain (DOPE-PEG$_{350}$), a cryoprotectant and precipitant of protein crystals. Upon reconstitution into a DOPE-PEG$_{350}$∥DOPA-supplemented asymmetric bilayer (Fig. 5A) the probability of finding the PM open was 0.61 ± 0.03, a value equal within error to that observed in DOPI∥DOPA containing bilayers. To dissect the contribution of PE from that of PEG$_{350}$ in the DOPE-PEG$_{350}$ headgroup, the PM was reconstituted in DPhPE∥DOPA-supplemented asymmetric bilayers (Fig. 5B). Under these conditions the P_o was drastically reduced to 0.04 ± 0.01 (a 15-fold decrement), indicating that PE has a marginal effect on channel activity. This finding is remarkable in two ways. First, PEGylation of PE, a doping lipid in which practically no channel activity was detected, retrieves a gain-of-function PM that is rarely closed. Second, given that PEG-350, with an estimated extended length of 1,400 Å and known ability to exclude water from the membrane-bulk solution interface (54), it follows that it is the shared ability of glycerol (51), inositol, and PEG to alter the water structure at the extracellular interface that is crucial to stabilize the open conformation of the PM.
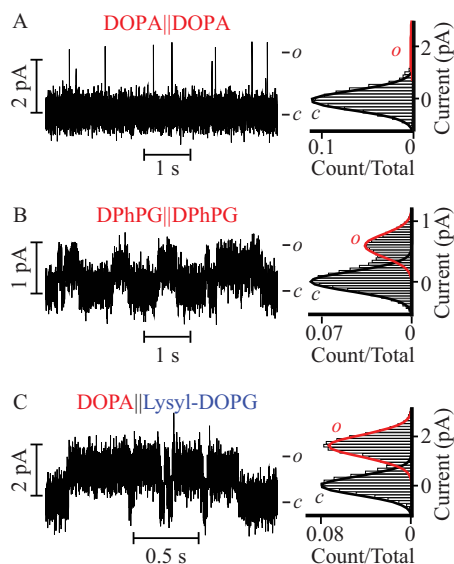
FIGURE 6. **The lipid-modulated stabilization of the PM open state occurs at physiological ionic strength.** Single channel steady-state current recordings (*left*) and their corresponding normalized all point histograms (*right*) of the PM in symmetric DPhPC bilayers supplemented with (*A*) DOPA and (*B*) DPhPG, and (*C*) in asymmetric bilayers doped with DOPA on the extracellular leaflet and lysyl-DOPG in the intracellular facing monolayer. All the recordings were acquired in 0.15 M KCl, 10 mM HEPES, pH 7.4, at V = 50 mV. Currents were further filtered to 300 Hz for analysis and presentation.

To validate this novel proposal we asked if the reported water-mediated lipid effect on the stability of the open conformation of the PM could be mimicked in a symmetric DOPA containing bilayer by supplementing the extracellular bathing solution (0.5 M KCl) with a cryoprotectant. In the presence of 1% (v/v) (0.17 M) ethylene glycol (Fig. 5C) or 0.2 M mannitol (Fig. 5D), the P_o and τ_{open} of the PM increased to 0.5 ± 0.1 and 14 ± 4 ms in ethylene glycol and 0.5 ± 0.1 and 8 ± 2 ms in mannitol, representing a gain of 25-fold in P_o and 8–14-fold in τ_{open} relative to the values observed in symmetric lipids bilayers bathed exclusively in 0.5 M KCl. Concomitant with this gain, there was a reduction in γ from 105 ± 4 to 45 ± 7 pS in ethylene glycol and 65 ± 5 pS in mannitol. From these results we conclude that the evoked destabilization of the water structure at the extracellular membrane-solution interface mediated by lipids with exposed hydroxyls is faithfully reproduced by supplementing the extracellular bulk solution with cryoprotectants. This is indicative of a role of water structure at the extracellular interface in modulating the stability of the open conducting conformation of the PM.

On the Modulation of KvLm PM Open Stability by Lipid Monolayers at Physiological Ionic Strength—The single channel currents presented thus far were recorded in 0.5 M KCl solutions. This experimental condition was set for two reasons: to focus on interactions shorter than the Debye length (4 Å) and to increase the signal-to-noise ratio and therefore resolve detailed features of the channel in different bilayer compositions and modalities. To explore if the reported gain in open conformation stability at high ionic strength (0.5 M), occurs at a physiological ionic strength, we acquired single channel currents in 0.15 M KCl, 10 mM HEPES, pH 7.4, in symmetric DOPA and DPhPG containing bilayers (Fig. 6, A and B), as well as in asymmetric bilayers containing DOPA on the extracellular facing leaflet and lysyl-DOPG in the intracellular facing monolayer (DOPA‖lysyl-DOPG, Fig. 6C). In symmetric DOPA containing bilayers the PM opened to the characteristic low P_o (0.02 ± 0.01), arising from short openings (τ_{open} = 0.9 ± 0.2 ms and burst length = 3 ± 1 ms) with γ = 35 ± 5 pS (Fig. 6A and Table 3). In contrast, in both DPhPG-doped symmetric bilayers and in DOPA‖lysyl-DOPG asymmetric bilayers, the PM opened to a high P_o and reduced γ: 0.35 ± 0.05 and 12 ± 5 pS in DPhPG-doped symmetric bilayers and 0.5 ± 0.1 and 30 ± 5 pS in DOPA‖lysyl-DOPG bilayers (Fig. 6, B and C, Table 3). Lower values of γ are consistent with a decreased concentration of current carrying species. In both types of bilayers, the ~17- and 25-fold increase in P_o came at the expense of an increase in τ_{open} and burst length: 10 ± 3 and 15 ± 5 ms in DPhPG-symmetric bilayers and 20 ± 3 and 40 ± 10 ms in DOPA‖lysyl-DOPG bilayers (Table 3). Since the P_o, τ_{open}, and characteristic burst length are observed to be equal within error (see Tables 1–3) at 0.15 and 0.5 M KCl in these three kinds of bilayers, we conclude that the lipid-mediated stabilization of the open conformation through a proposed change in water structure at the extracellular face of the PM happens at physiological ionic strength.

On the Modulation of KvLm PM Single Channel Conductance by Lipid Monolayers—The measured PM γ in symmetric bilayers can be pooled into three groups: low γ (10 ± 2 pS), intermediate γ (50 ± 10 pS), and high γ (105 ± 4 pS) (Table 1). At the extremes are the γ values measured in bilayers containing a terminal positively charged group (lysyl-DOPG, 10 ± 2 pS), and a terminal negatively charged moiety (DOPA, 105 ± 4 pS). In the negatively charged lyso-PG, DPhPG, DOPG, and DOPI containing bilayers, as well as in neutral monoolein membranes, γ was equal within error and averaged to 50 ± 10 pS.

In asymmetric membranes, the γ values can again be grouped according to average magnitude: intermediate γ (55 ± 10 pS) and high γ (90 ± 10 pS) (Table 2). High γ was measured in bilayers in which DOPA was present in the extracellular leaflet: 74 ± 4 pS in DOPA‖DPhPG, 94 ± 3 pS in DOPA‖DOPI, and 92 ± 7 pS in DOPA‖lysyl-DOPG. In contrast, an intermediate γ was measured in bilayers where DOPA was located on the intracellular leaflet: 50 ± 5 pS in DPhPG‖DOPA, 70 ± 4 pS in DOPI‖DOPA, 46 ± 2 pS in Lysyl-DOPG‖DOPA, and 55 ± 5 pS in PEG$_{350}$‖DOPA. From these results we conclude that in asymmetric bilayers, the presence of DOPA at the extracellular leaflet is the primary determinant of a high outward γ, which is largely independent of the charge and chemical composition of the doping lipid headgroup in the intracellular leaflet. The extent of the contribution of the lipid identity to the single channel conductance (high at the extracellular, low at the intracellular) is consistent with the fact that the extracellular PM gate located at the selectivity filter is exposed to the lipid composition (PDB code 4H33) (5), whereas the PM gate located at the bundle crossing is mostly insulated from the lipid bilayer by the outer helix and S4–S5 linker (5). In addition, the minor effect of the lipid monolayer surface-charge reported is argued to be a result of charge screening by the high ionic strength of the solution bathing the bilayers (14, 15, 19).

TABLE 3

Single channel properties of the PM in symmetric and asymmetric DPhPC lipid bilayers supplemented with the indicated lipids recorded in 0.15 M KCl at V = 50 mV

Experimental conditions (Filter∥bundle)	γ	P_o	τ_{open}	Burst length	N
	pS		*ms*	*ms*	*n*
DOPA∥DOPA	35 ± 5	0.02 ± 0.01	0.9 ± 0.2	3 ± 1	3,230
					3
DPhPG∥DPhPG	12 ± 5	0.35 ± 0.05	10 ± 3	15 ± 5	5,847
					3
DOPA∥lysyl-DOPG	30 ± 5	0.5 ± 0.1	20 ± 5	40 ± 10	6,599
					3

DISCUSSION

The results here documented outline a deterministic role of the lipid monolayer headgroup on the stability of the open conformation of a Kv pore module in the absence of the voltage-sensing modules. This finding is novel. It posits that the impact of the lipid bilayer in modulating Kv channel function is not solely centered on an interaction with the voltage sensor, as previously suggested (22, 24, 25). Importantly, it identifies the composition of the monolayer surrounding the filter gate as the primary determinant of the lipid-induced stabilization of the open PM conformation. It also provides further support for the notion that the function of Kv channels can only be compared if the functional assay is performed on lipid bilayers of the same composition (33). The implication is that the lipid bilayer and, as determined here, the lipid monolayer is effectively a regulatory module that contributes to the functional diversity observed in Kv channels. It implies that the same Kv channel may operate significantly differently when expressed in different cellular contexts, compartments, or species (13, 20, 24, 33, 55). But how does the lipid monolayer achieve this modulating role?

The Proposed Functional Coupling between Lysyl on the Cytoplasmic Facing Monolayer and Phe-19 Is Not Specific to KvLM—In KvLm, the first hydrophobic residue in the string of hydrophobic residues that constitutes the outer helix (S5) of the PM is a phenylalanine (Phe-19). The data lead us to propose that the observed increase in the stability of the open conformation of the PM in lysyl-DOPG containing bilayers arises from a π-cation interaction between Phe-19 in the PM and the lysyl moiety on the cytoplasm facing lipid monolayer, presumably established in the open conformation of the channel. Analysis of an alignment of 85 Kv channel sequences of bacterial origin shows that phenylalanine occupies the same position (5th amino acid in S5) in 36 sequences (42%) (8). This direct coupling effect is, therefore, presumably not specific to KvLm and of importance for the design of novel channels in the context of their lipid bilayer environment, which together may be tuned to generate *a la carte* biological transistors. In addition, from a protein design perspective, the sequence motif of an Arg-Phe at the start of the hydrophobic stretch in the outer helix appears amenable to act as a "molecular micro-switch" (56, 57) in the gating process. When facing a positive charge, a simple 90° rotation allows for an attractive or repulsive interaction.

Hypothesis on How a Change in Water Structure at the Membrane-Solution Interface Modulates Gating of the PM—The results indicate that a layer of hydroxyl groups exposed on the extracellular monolayer of the bilayer as generated by anchoring the cryoprotectants glycerol, inositol, or PEG, stabilizes the open conformation of the PM. This is significant in that it identifies the composition of the extracellular membrane-solution interface, a region predicted to be no deeper than ~4 Å, the Debye length at 0.5 M monovalent salt, as a determinant in the stabilization of the open conformation. The underlying basis for this effect is proposed to be an alteration of water structure at the membrane interface, a property that is shared by all cryoprotectants. If our line of reasoning were correct, which bilayer properties change and how are such changes transmitted to the pore? Admittedly, this is currently unknown. However, a lack of miscibility with water has been theoretically correlated with the exclusion of water from glycerol-rich domains (51). Because PG headgroups position their glycerol terminal moieties in plane with the membrane interface at the same depth as the lipid phosphate group (plane *b*, Fig. 1) (58), a layer of glycerol would be predicted to alter the water structure at such an interface (52, 53). We conjecture that this interfacial layer represents the effective aqueous-hydrophobic boundary (59). Accordingly, water exclusion from such an interface could stabilize the PM open state in at least two ways: through a depletion of water at the exit from the permeation path or at the protein surface. The first path would attenuate the dissociation rate of K$^+$ from the outermost binding site (S0) of the selectivity filter, given that the water required to replace the carbonyls and solvate the ion would be presumably scarce. A delayed exit from the filter would generate longer openings of reduced conductance, in analogy to what is observed when K$^+$ is replaced by Rb$^+$ as the charge carrier (8, 60). This proposal may be more relevant for KvLm than for other Kv channels, given that the extracellular loop connecting the outer and pore helices in KvLm is short (5), and therefore does not create a major barrier between ionic concentration at the membrane surface and at the channel surface, near the S0 ion binding site in the filter gate (61). A direct effect of water on the structure of the channel protein through a modulation of hydrogen bonds, as recently outlined for KcsA, a K$^+$ channel that inactivates quickly (62), cannot be excluded. These proposals remain to be validated.

Recently, we demonstrated a comparable stabilization of the open conformation of the PM by positioning a steric lid (imipramine, charybdotoxin, or fluorescein-maleimide) over the exit of the permeation path located at the filter gate; an effect that we attributed to an increase in the contact time between filter gate and permeant ion (45). This reasoning also explains the results of this study. We conjecture that a depletion of available water at the exit of the permeation path acts as a liquid lid by making rehydration of an ion exiting the filter gate less favorable, thereby lengthening the association time between permeant ion and filter gate. Together, the results indicate that in a

PM that can transit between open and closed at 0 mV (5), the stabilization of the open conformation of the channel depends stringently on the prolonged residency of permeant ions at the filter gate.

In conclusion, we have demonstrated that the lipid monolayer *per se* is a functional module that is coupled to the pore module in a PM specific manner. The realization that both single channel conductance and probability of finding the channel open (the two values determining the overall outward current) are largely determined by monolayer composition shows another means by which nature has fitted the function of channels to their environment. The demonstration that the conversion of a PM that rarely opens to a conductor that rarely closes occurs in an atypical asymmetric membrane (40, 63), containing lysyl-DOPG at the bundle (DOPA‖Lysyl-DOPG) or DOPI at the filter (DOPI‖DOPA) provides another plausible reason why nature settled on specific lipid monolayer composition and bilayer asymmetry.

REFERENCES

1. Montal, M. (1990) Molecular anatomy and molecular design of channel proteins. *FASEB J.* **4,** 2623–2635
2. Bezanilla, F. (2000) The voltage sensor in voltage-dependent ion channels. *Physiol. Rev.* **80,** 555–592
3. Long, S. B., Campbell, E. B., and Mackinnon, R. (2005) Crystal structure of a mammalian voltage-dependent Shaker family K⁺ channel. *Science* **309,** 897–903
4. Long, S. B., Tao, X., Campbell, E. B., and MacKinnon, R. (2007) Atomic structure of a voltage-dependent K⁺ channel in a lipid membrane-like environment. *Nature* **450,** 376–382
5. Santos, J. S., Asmar-Rovira, G. A., Han, G. W., Liu, W., Syeda, R., Cherezov, V., Baker, K. A, Stevens, R. C., and Montal, M. (2012) Crystal structure of a voltage-gated K⁺ channel pore module in a closed state in lipid membranes. *J. Biol. Chem.* **287,** 43063–43070
6. Chakrapani, S., Cuello, L. G., Cortes, D. M., and Perozo, E. (2008) Structural dynamics of an isolated voltage-sensor domain in a lipid bilayer. *Structure* **16,** 398–409
7. Butterwick, J. A., and MacKinnon, R. (2010) Solution structure and phospholipid interactions of the isolated voltage-sensor domain from KvAP. *J. Mol. Biol.* **403,** 591–606
8. Santos, J. S., Grigoriev, S. M., and Montal, M. (2008) Molecular template for a voltage sensor in a novel K⁺ channel. III. Functional reconstitution of a sensorless pore module from a prokaryotic Kv channel. *J. Gen. Physiol.* **132,** 651–666
9. Alabi, A. A., Bahamonde, M. I., Jung, H. J., Kim, J. I., and Swartz, K. J. (2007) Portability of paddle motif function and pharmacology in voltage sensors. *Nature* **450,** 370–375
10. Syeda, R., Santos, J. S., Montal, M., and Bayley, H. (2012) Tetrameric assembly of KvLm K⁺ channels with defined numbers of voltage sensors. *Proc. Natl. Acad. Sci. U.S.A.* **109,** 16917–16922
11. Santos, J. S., Lundby, A., Zazueta, C., and Montal, M. (2006) Molecular template for a voltage sensor in a novel K⁺ channel. I. Identification and functional characterization of KvLm, a voltage-gated K⁺ channel from *Listeria monocytogenes*. *J. Gen. Physiol.* **128,** 283–292
12. Lundby, A., Santos, J. S., Zazueta, C., and Montal, M. (2006) Molecular template for a voltage sensor in a novel K⁺ channel. II. Conservation of a eukaryotic sensor fold in a prokaryotic K⁺ channel. *J. Gen. Physiol.* **128,** 293–300
13. Forte, M., Satow, Y., Nelson, D., and Kung, C. (1981) Mutational alteration of membrane phospholipid composition and voltage-sensitive ion channel function in paramecium. *Proc. Natl. Acad. Sci. U.S.A.* **78,** 7195–7199
14. Bell, J. E., and Miller, C. (1984) Effects of phospholipid surface charge on ion conduction in the K⁺ channel of sarcoplasmic reticulum. *Biophys. J.* **45,** 279–287
15. Moczydlowski, E., Alvarez, O., Vergara, C., and Latorre, R. (1985) Effect of phospholipid surface charge on the conductance and gating of a Ca²⁺-activated K⁺ channel in planar lipid bilayers. *J. Membr. Biol.* **83,** 273–282
16. Bian, J., Cui, J., and McDonald, T. V. (2001) HERG K⁺ channel activity is regulated by changes in phosphatidylinositol 4,5-bisphosphate. *Circ. Res.* **89,** 1168–1176
17. Alvis, S. J., Williamson, I. M., East, J. M., and Lee, A. G. (2003) Interactions of anionic phospholipids and phosphatidylethanolamine with the potassium channel KcsA. *Biophys. J.* **85,** 3828–3838
18. Zhang, H., Craciun, L. C., Mirshahi, T., Rohács, T., Lopes, C. M., Jin, T., and Logothetis, D. E. (2003) PIP₂ activates KCNQ channels, and its hydrolysis underlies receptor-mediated inhibition of M currents. *Neuron* **37,** 963–975
19. Park, J. B., Kim, H. J., Ryu, P. D., and Moczydlowski, E. (2003) Effect of phosphatidylserine on unitary conductance and Ba²⁺ block of the BK Ca²⁺-activated K⁺ channel. Re-examination of the surface charge hypothesis. *J. Gen. Physiol.* **121,** 375–397
20. Oliver, D., Lien, C. C., Soom, M., Baukrowitz, T., Jonas, P., and Fakler, B. (2004) Functional conversion between A-type and delayed rectifier K⁺ channels by membrane lipids. *Science* **304,** 265–270
21. Lee, S. Y., Lee, A., Chen, J., and MacKinnon, R. (2005) Structure of the KvAP voltage-dependent K⁺ channel and its dependence on the lipid membrane. *Proc. Natl. Acad. Sci. U.S.A.* **102,** 15441–15446
22. Schmidt, D., Jiang, Q. X., and MacKinnon, R. (2006) Phospholipids and the origin of cationic gating charges in voltage sensors. *Nature* **444,** 775–779
23. Marius, P., Zagnoni, M., Sandison, M. E., East, J. M., Morgan, H., and Lee, A. G. (2008) Binding of anionic lipids to at least three nonannular sites on the potassium channel KcsA is required for channel opening. *Biophys. J.* **94,** 1689–1698
24. Schmidt, D., and MacKinnon, R. (2008) Voltage-dependent K⁺ channel gating and voltage sensor toxin sensitivity depend on the mechanical state of the lipid membrane. *Proc. Natl. Acad. Sci. U.S.A.* **105,** 19276–19281
25. Xu, Y., Ramu, Y., and Lu, Z. (2008) Removal of phospho-head groups of membrane lipids immobilizes voltage sensors of K⁺ channels. *Nature* **451,** 826–829
26. Whorton, M. R., and MacKinnon, R. (2011) Crystal structure of the mammalian GIRK2 K⁺ channel and gating regulation by G proteins, PIP2, and sodium. *Cell* **147,** 199–208
27. Iwamoto, M., and Oiki, S. (2013) Amphipathic antenna of an inward rectifier K⁺ channel responds to changes in the inner membrane leaflet. *Proc. Natl. Acad. Sci.* **110,** 749–754
28. Rodriguez-Menchaca, A. A., Adney, S. K., Tang, Q.-Y., Meng, X.-Y., Rosenhouse-Dantsker, A., Cui, M., and Logothetis, D. E. (2012) PIP2 controls voltage-sensor movement and pore opening of Kv channels through the S4-S5 linker. *Proc. Natl. Acad. Sci. U.S.A.* **109,** E2399–408
29. Zaydman, M. A, Silva, J. R., Delaloye, K., Li, Y., Liang, H., Larsson, H. P., Shi, J., and Cui, J. (2013) Kv7.1 ion channels require a lipid to couple voltage sensing to pore opening. *Proc. Natl. Acad. Sci. U.S.A.* **110,** 13180–13185
30. Weingarth, M., Prokofyev, A., van der Cruijsen, E. A., Nand, D., Bonvin, A. M., Pongs, O., and Baldus, M. (2013) Structural determinants of specific lipid binding to potassium channels. *J. Am. Chem. Soc.* **135,** 3983–3988
31. van der Cruijsen, E. A., Nand, D., Weingarth, M., Prokofyev, A., Hornig, S., Cukkemane, A. A., Bonvin, A. M., Becker, S., Hulse, R. E., Perozo, E., Pongs, O., and Baldus, M. (2013) Importance of lipid-pore loop interface for potassium channel structure and function. *Proc. Natl. Acad. Sci. U.S.A.* **110,** 13008–13013
32. van Dalen, A., and de Kruijff, B. (2004) The role of lipids in membrane insertion and translocation of bacterial proteins. *Biochim. Biophys. Acta* **1694,** 97–109
33. Schmidt, D., Cross, S. R., and MacKinnon, R. (2009) A gating model for the archeal voltage-dependent K⁺ channel KvAP in DPhPC and POPE:POPG decane lipid bilayers. *J. Mol. Biol.* **390,** 902–912
34. Hoshi, T., Zagotta, W. N., and Aldrich, R. W. (1991) Two types of inactivation in Shaker K⁺ channels. Effects of alterations in the carboxy-terminal region. *Neuron* **7,** 547–556
35. Choi, K. L., Aldrich, R. W., and Yellen, G. (1991) Tetraethylammonium blockade distinguishes two inactivation mechanisms in voltage-activated K⁺ channels. *Proc. Natl. Acad. Sci. U.S.A.* **88,** 5092–5095

36. Liu, Y., Jurman, M. E., and Yellen, G. (1996) Dynamic rearrangement of the outer mouth of a K$^+$ channel during gating. *Neuron* **16,** 859–867

37. Liu, Y., Holmgren, M., Jurman, M. E., and Yellen, G. (1997) Gated access to the pore of a voltage-dependent K$^+$ channel. *Neuron* **19,** 175–184

38. Montal, M. (1973) Asymmetric lipid bilayers response to multivalent ions. *Biochim. Biophys. Acta* **298,** 750–754

39. Rothman, J. E., and Kennedy, E. P. (1977) Asymmetrical distribution of phospholipids in the membrane of *Bacillus megaterium. J. Mol. Biol.* **110,** 603–618

40. Op den Kamp, J. A. (1979) Lipid asymmetry in membranes. *Annu. Rev. Biochem.* **48,** 47–71

41. Devaux, P. F., and Morris, R. (2004) Transmembrane asymmetry and lateral domains in biological membranes. *Traffic* **5,** 241–246

42. van Meer, G., Voelker, D. R., and Feigenson, G. W. (2008) Membrane lipids. Where they are and how they behave. *Nat. Rev. Mol. Cell Biol.* **9,** 112–124

43. Ma, J. C., and Dougherty, D. A. (1997) The cation-π interaction. *Chem. Rev.* **97,** 1303–1324

44. Valiyaveetil, F. I., Zhou, Y., and MacKinnon, R. (2002) Lipids in the structure, folding, and function of the KcsA K$^+$ channel. *Biochemistry* **41,** 10771–10777

45. Santos, J. S., Syeda, R., and Montal, M. (2013) Stabilization of the conductive conformation of a Kv channel. The lid mechanism. *J. Biol. Chem.* **288,** 16619–16628

46. Bayley, H., Cronin, B., Heron, A., Holden, M. A., Hwang, W. L., Syeda, R., Thompson, J., and Wallace, M. (2008) Droplet interface bilayers. *Mol. Biosyst.* **4,** 1191–1208

47. Qin, F. (2004) Restoration of single-channel currents using the segmental k-means method based on hidden Markov modeling. *Biophys. J.* **86,** 1488–1501

48. Krieger, E., Darden, T., Nabuurs, S. B., Finkelstein, A., and Vriend, G. (2004) Making optimal use of empirical energy functions. Force-field parameterization in crystal space. *Proteins* **57,** 678–683

49. Duan, Y., Wu, C., Chowdhury, S., Lee, M. C., Xiong, G., Zhang, W., Yang, R., Cieplak, P., Luo, R., Lee, T., Caldwell, J., Wang, J., and Kollman, P. (2003) A point-charge force field for molecular mechanics simulations of proteins based on condensed-phase quantum mechanical calculations. *J. Comput. Chem.* **24,** 1999–2012

50. McGaughey, G. B., Gagné, M., and Rappé, A. K. (1998) π-Stacking interactions. *J. Biol. Chem.* **273,** 15458–15463

51. Towey, J. J., Soper, A. K., and Dougan, L. (2012) Molecular insight into the hydrogen bonding and micro-segregation of a cryoprotectant molecule. *J. Phys. Chem. B* **116,** 13898–13904

52. Zhao, W., Róg, T., Gurtovenko, A. A., Vattulainen, I., and Karttunen, M. (2007) Atomic-scale structure and electrostatics of anionic palmitoyl-oleoylphosphatidylglycerol lipid bilayers with Na$^+$ counterions. *Biophys. J.* **92,** 1114–1124

53. Murzyn, K., Zhao, W., Karttunen, M., Kurdziel, M., and Róg, T. (2006) Dynamics of water at membrane surfaces. Effect of headgroup structure. *Biointerphases* **1,** 98–105

54. Tirosh, O., Barenholz, Y., Katzhendler, J., and Priev, A. (1998) Hydration of polyethylene glycol-grafted liposomes. *Biophys. J.* **74,** 1371–1379

55. Schmidt, D., del Mármol, J., and MacKinnon, R. (2012) Mechanistic basis for low threshold mechanosensitivity in voltage-dependent K$^+$ channels. *Proc. Natl. Acad. Sci. U.S.A.* **109,** 10352–10357

56. Holst, B., Nygaard, R., Valentin-Hansen, L., Bach, A., Engelstoft, M. S., Petersen, P. S., Frimurer, T. M., and Schwartz, T. W. (2010) A conserved aromatic lock for the tryptophan rotameric switch in TM-VI of seven-transmembrane receptors. *J. Biol. Chem.* **285,** 3973–3985

57. Nygaard, R., Frimurer, T. M., Holst, B., Rosenkilde, M. M., and Schwartz, T. W. (2009) Ligand binding and micro-switches in 7TM receptor structures. *Trends Pharmacol. Sci.* **30,** 249–259

58. Pan, J., Heberle, F. A., Tristram-Nagle, S., Szymanski, M., Koepfinger, M., Katsaras, J., and Kučerka, N. (2012) Molecular structures of fluid phase phosphatidylglycerol bilayers as determined by small angle neutron and x-ray scattering. *Biochim. Biophys. Acta* **1818,** 2135–2148

59. Montal, M. (1976) Experimental membranes and mechanisms of bioenergy transductions. *Annu. Rev. Biophys. Bioeng.* **5,** 119–175

60. Swenson, R. P., Jr., and Armstrong, C. M. (1981) K+ channels close more slowly in the presence of external K$^+$ and Rb$^+$. *Nature* **291,** 427–429

61. Zhou, Y., and MacKinnon, R. (2003) The occupancy of ions in the K$^+$ selectivity filter. Charge balance and coupling of oon binding to a protein conformational change underlie high conduction rates. *J. Mol. Biol.* **333,** 965–975

62. Ostmeyer, J., Chakrapani, S., Pan, A. C., Perozo, E., and Roux, B. (2013) Recovery from slow inactivation in K$^+$ channels is controlled by water molecules. *Nature* **501,** 121–124

63. Fischer, W., and Leopold, K. (1999) Polar lipids of four Listeria species containing L-lysylcardiolipin, a novel lipid structure, and other unique phospholipids. *Int. J. Syst. Bacteriol.* **49,** 653–662